Available online at www.sciencedirect.com
ScienceDirect
Journal of Sound and Vibration 318 (2008) 1–17
JOURNAL OF SOUND AND VIBRATION
www.elsevier.com/locate/jsvi

Review

Dynamics studies of a flexible hub–beam system with significant damping effect

Guo-Ping Cai[a,*], C.W. Lim[b]

[a]Department of Engineering Mechanics, Shanghai Jiaotong University, Shanghai 200240, PR China
[b]Department of Building and Construction, City University of Hong Kong, Tat Chee Avenue, Kowloon, Hong Kong, PR China

Received 19 January 2008; received in revised form 16 April 2008; accepted 4 June 2008
Handling Editor: L.G. Tham
Available online 11 July 2008

Abstract

In this paper, dynamics of a flexible hub–beam system is studied using a first-order approximation coupling (FOAC) model and the assumed mode discretization method. Three kinds of damping are considered: structural damping of beam material, air damping caused by large motion of the system, and damping located at hub bearing. Validity of the FOAC model is verified by numerical simulations under two cases: (i) known large motion of system and (ii) unknown large motion of system. Damping may significantly affect system dynamics and should not be neglected for high-speed large motion of system or highly flexible beam.

Contents

*Corresponding author.
E-mail addresses: caigp@sjtu.edu.cn (G.-P. Cai), bccwlim@cityu.edu.hk (C.W. Lim).

0022-460X/$ - see front matter © 2008 Elsevier Ltd. All rights reserved.
doi:10.1016/j.jsv.2008.06.009

1. Introduction

It is well known that flexible hub–beam system has many applications in many high-tech engineering area, such as aerospace, aviation, and robotics. Studies on flexible hub–beam system can be classified into two categories: modelling theory and control study. For the study of modelling theory, the traditional model assumes small deformation in structural dynamics where axial and transverse displacements at any point in the beam are uncoupled, and the dynamic model established based on this small deformation assumption is referred as the zeroth-order approximation coupling (ZOAC) model. This model is widely used in dynamic analysis of rigid–flexible coupling dynamic systems in past decades [1–6]. In 1987, Kane [3] investigated a rotating flexible cantilever beam using the traditional ZOAC model, and showed that this model fails to describe dynamic behaviour of the beam when the beam is in high rotation speed. Dynamic stiffening phenomenon was first pointed out in Ref. [3]. Since then, most studies on rigid–flexible coupling dynamic systems are focused on the investigation of dynamic stiffening, and many methodologies are developed to capture dynamic stiffening term in dynamic systems [7–9]. The introduction of dynamic stiffening indicates that there still exist big limitations on understanding of dynamics mechanism of rigid–flexible coupling systems, and on accuracy of mathematical model established to describe dynamic behaviour of the systems. Meanwhile, it also promotes extensive research on modelling of rigid–flexible coupling dynamic systems. Recently, based on the theory of continuum medium mechanics and the theory of analysis dynamics, and with consideration of the second-order coupling term of axial displacement caused by transverse displacement of flexible beam, the first-order approximation coupling (FOAC) model is developed for flexible hub–beam system [10–13]. Physical explanation to dynamic stiffening is suggested in Refs. [10–13] by using the FOAC model. Dynamic stiffening is essentially a structural dynamic problem in non-inertial system, which results from additional stiffness caused by the coupling of large rotation motion of rigid hub and small elastic vibration of flexible beam [10–13]. In addition, existence of dynamic stiffening and validity of the FOAC model are experimentally verified in Refs. [10–12].

For modelling of flexible hub–beam system, dynamic equation obtained by the Hamilton theory is a partial differential and integral equations which are nonlinear, time-varying and strongly coupling. It is generally impossible to get analytical solutions to these equations. For convenience in analysis, discretization of equations is generally required. Finite element method (FEM) and assumed mode method (AMM) are often used as discretization method of equations. For active control studies of flexible hub–beam system, degree of freedom of dynamic model obtained by using FEM is usually very large and active controller requires system states being used in control feedback, so dynamic model by FEM is not convenient for control design and control implementation. Therefore, AMM is often used for control study. In fact for dynamics and control of flexible hub–beam, FEM is usually available for dynamic analysis of the system and AMM is available for control study.

On the other hand, damping exists inevitably in flexible hub–beam system. There exists not only structural damping caused by beam material but also air damping by large motion of beam, and damping by rotation bearing of hub as well. In existing studies for flexible hub–beam system, damping is often not taken into account because modelling work will become very complicated. But for some cases damping has great effect on system dynamics and may not be neglected. For example, when rotation speed of flexible hub–beam system is high and flexibility of the beam is large, damping force caused by air will have great effect on system dynamics and should be considered in modelling. In Ref. [10], structural damping, air damping, and damping of hub bearing are considered in modelling for flexible hub–beam system, and validity of the FOAC model is experimentally verified as well. However, discretization method adopted in Ref. [10] is FEM and AMM is not studied.

In this paper, modelling theory for flexible hub–beam system is studied by using AMM for discretization. Structural damping, air damping and bearing damping of hub are considered in the modelling. Contributions of the three damping to dynamic equation are formulated by using the Hamilton theory. The FOAC model based on AMM is presented considering effect of damping. Dynamic model in non-inertial system is presented too. The FOAC model based on AMM is validated and effect of damping on system dynamics is investigated through numerical simulations.

This paper is organized as follows. Section 2 first briefly presents expression of the FOAC model for flexible hub–beam system by the Hamilton theory and using AMM for discretization with and without damping.

Dynamic model in non-inertial system is given in Section 3. Section 4 presents simulation and comparison studies using the FOAC model and AMM. Two cases are considered: (i) known and (ii) unknown large motion of system. Finally, a concluding remark is given in Section 5.

2. Dynamic model

2.1. The first-order approximation dynamic model

A hub–beam rotating in the horizontal plane is considered here as shown in Fig. 1, where the hub is a rigid body and the beam is a flexible one. The global coordinate system $O_0{-}X_0Y_0$ is the inertial system. The local coordinate system $O{-}XY$ is fixed to the beam. One end of the beam is fixed to the hub. The hub rotates in the horizontal plane and the beam rotates about the hub. Large rotating motion of the hub forms a non-inertial field and the beam vibrates in this field due to its elasticity and inertia. Effect of gravity of the hub and the beam is neglected. Properties of the flexible beam are represented as follows: L is the length of beam, E Young's modulus of beam, I the area moment of inertia of beam cross-section, ρ the mass per unit volume, and A the cross-section area. Radius of the hub is represented by r_A and τ is the external rotating torque acted on the hub. The parameter θ is the angular rotation of hub.

Fig. 2 illustrates deformation at an arbitrary point P_0 of the beam, where x is the unreformed location of P_0. After deformation, P_0 moves to the point P. The location vector of point P in the $O_0{-}X_0Y_0$ system is represented by $\mathbf{r}_P$ and is given by

$$\mathbf{r}_P = \mathbf{r}_A + \mathbf{\Theta}(\mathbf{r}_0 + \mathbf{r}_1) \tag{1}$$

where $\mathbf{r}_A$ is the location vector of origin O of the $O{-}XY$ system in the $O_0{-}X_0Y_0$ system; and $\mathbf{\Theta}$ is the direction cosine matrix that is the $O{-}XY$ system with respect to the $O_0{-}X_0Y_0$ system, which is given by

$$\mathbf{\Theta} = \begin{bmatrix} \cos\theta & -\sin\theta \\ \sin\theta & \cos\theta \end{bmatrix}.$$

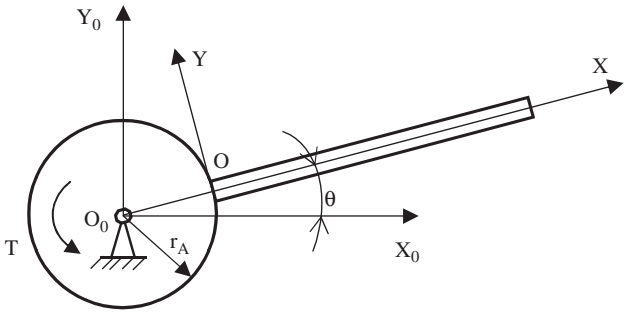

Fig. 1. Structural model of a hub–beam system.

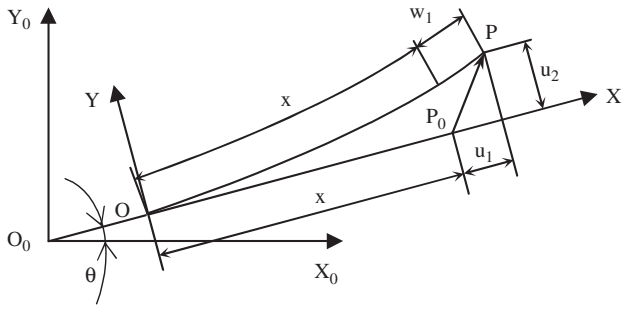

Fig. 2. Deformation description of a flexible cantilever beam.

The vector $\mathbf{r}_0$ is the location vector of point P_0 in the $O-XY$ system and its coordinate is given by $[x, \quad 0]^{\mathrm{T}}$, where the superscript T indicates the transpose of a vector or matrix, and $\mathbf{r}_1$ the deformation vector of P_0 in the $O-XY$ system and its coordinate is represented by $\left[u_1(x,t), \quad u_2(x,t)\right]^{\mathrm{T}}$, which can be written as [10,13]

$$\mathbf{r}_1 = \begin{bmatrix} u_1(x,t) \\ u_2(x,t) \end{bmatrix} = \begin{bmatrix} w_1(x,t) + w_c(x,t) \\ w_2(x,t) \end{bmatrix} = \begin{bmatrix} w_1(x,t) - \frac{1}{2}\int_0^x \left(\frac{\partial w_2(\xi,t)}{\partial \xi}\right)^2 \mathrm{d}\xi \\ w_2(x,t) \end{bmatrix} \tag{2}$$

where $w_1(x,\ t)$ is the axial extension quantity and $w_2(x,\ t)$ is the transverse displacement. For a slender beam, $w_2(x,\ t)$ is generally much larger than $w_1(x,\ t)$, thus it is reasonable to assume $w_2(x,\ t) = u_2(x,\ t)$. The parameter $w_c(x,t) = -1/2\int_0^x ((\partial w_2(\xi,t))/(\partial \xi))^2\,\mathrm{d}\xi$ is the second-order coupling term that is axial shrinking quantity caused by $w_2(x,\ t)$. In the ZOAC model, small deformation assumption in structural dynamics is adopted, so $u_1(x,\ t) = w_1(x,\ t)$ is assumed, i.e., $w_c(x,\ t)$ is not taken into account in the modelling. Because the object of structural dynamics is for a structure with no rotation, neglecting the effect of $w_c(x,\ t)$ on system stiffness in the modelling is reasonable. But for flexible hub–beam system with large rotation and when rotating motion is at high speed, $w_c(x,\ t)$ will have significant effect on system performance and should be considered in the modelling. This has been demonstrated by numerical simulation and experimental study in Refs. [10–13].

Kinetic energy of the system can be expressed as

$$T = \frac{1}{2}J_H\dot{\theta}^2 + \frac{1}{2}\int_0^L \rho A \dot{\mathbf{r}}_P^{\mathrm{T}}\dot{\mathbf{r}}_P\,\mathrm{d}x \tag{3}$$

where J_H is the rotary inertia of the hub. The parameter $\dot{\mathbf{r}}_P$ can be obtained by taking the first derivative in Eq. (1) as

$$\dot{\mathbf{r}}_P = \dot{\mathbf{r}}_A + \dot{\mathbf{\Theta}}(\mathbf{r}_0 + \mathbf{r}_1) + \mathbf{\Theta}\dot{\mathbf{r}}_1 \tag{4}$$

Potential energy of the system can be written as

$$H = \frac{1}{2}\int_0^L EA[w_1'(x,t)]^2\,\mathrm{d}x + \frac{1}{2}\int_0^L EI[w_2''(x,t)]^2\,\mathrm{d}x \tag{5}$$

where w_1' and w_2'' represents the first and second partial derivative with respect to x, respectively.

From Eqs. (3) and (5), the variations δT and δH can be computed. The work done by the external load is that by the rotational torque τ, which can be expressed as

$$\delta W_F = \tau\delta\theta \tag{6}$$

Using the Hamilton theory $\int_{t_1}^{t_2}(\delta T - \delta H + \delta W_F)\,\mathrm{d}t = 0$, the dynamics equation of system in partial differential form can be obtained as [10,13]

$$\int_0^L \{\rho A\ddot{w}_1 - 2\rho A\dot{\theta}\dot{w}_2 - \rho A\ddot{\theta}w_2 - \rho A\dot{\theta}^2(r_A + x + w_1) - EAw_1''\}\,\mathrm{d}x = 0 \tag{7}$$

$$\int_0^L \left\{\rho A\ddot{w}_2 + 2\rho A\dot{\theta}\dot{w}_1 + \rho A\ddot{\theta}(r_A + x + w_1) - \rho A\dot{\theta}^2 w_2 + EIw_2'' + \rho A\frac{\partial}{\partial x}\left[w_2'\int_x^L B(\xi,t)\,\mathrm{d}\xi\right]\right\}\mathrm{d}x = 0 \tag{8}$$

$$J_H\ddot{\theta} + \int_0^L \rho A\{\ddot{\theta}[(r_A + x)^2 + w_1^2 + w_2^2 + 2(r_A + x)(w_1 + w_c)] + (r_A + x + w_1)\ddot{w}_2 - w_2\ddot{w}_1 + 2\dot{\theta}[(r_A + x)(\dot{w}_1 + \dot{w}_c) + w_1\dot{w}_1 + w_2\dot{w}_2]\}\,\mathrm{d}x = \tau \tag{9}$$

Boundary conditions of the beam are as follows:

$$\begin{cases} w_1(0,t) = 0, \quad w_2(0,t) = 0, \quad w_1'(0,t) = 0, \quad EIw_2''(L,t) = 0, \\ EAw_1'(L,t) = 0, \quad EIw_2'''(L,t) = 0 \end{cases} \tag{10}$$

where $B(x, t)$ in Eq. (8) can be expressed as [10,13]

$$B(x,t) = -\dot{\theta}^2(r_A + x + w_1 + w_c) - 2\dot{\theta}\dot{w}_2 + \ddot{w}_1 + \ddot{w}_c - \ddot{\theta}w_2 \tag{11}$$

2.2. The assumed mode discretization method

Eqs. (7)–(9) are the partial differential and integral equations that are nonlinear, time-varying and strongly coupling. It is generally impossible to obtain analytical solutions to these equations. The idiomatic process method is to discretize these equations, i.e., to change the system from an infinite degree-of-freedom system into a finite degree-of-freedom system. Then an approximate solution to the original system is obtained from the corresponding finite degree-of-freedom system. AMM and FEM are the two methods that are often used as discretization methods for these equations. Because degree of freedom of dynamic model obtained using FEM is usually very large, which is not convenient for control design, AMM is used in this paper for discretization of Eqs. (7)–(9). In fact, for dynamics and control of rigid–flexible coupling systems, FEM is often used for study of dynamic behaviour of the systems, while AMM is often used for active control design.

The axial displacement w_1 and the transverse displacement w_2 of any point in the beam may be written as

$$w_1(x,t) = \mathbf{\Phi}_1(x)\mathbf{q}_1(t), \quad w_2(x,t) = \mathbf{\Phi}_2(x)\mathbf{q}_2(t) \tag{12}$$

where both $\mathbf{\Phi}_1(x)$ and $\mathbf{\Phi}_2(x)$ are $1 \times n$ vectors, representing mode functions of axial and transverse vibrations of the beam, respectively; and both $\mathbf{q}_1(t)$ and $\mathbf{q}_2(t)$ are $n \times 1$ vectors, representing modal coordinates of axial and transverse vibrations of the beam, respectively; which are given by

$$\mathbf{\Phi}_1(x) = [\phi_1^{(1)}(x), \phi_2^{(1)}(x), \ldots, \phi_n^{(1)}(x)], \quad \mathbf{q}_1(t) = [q_1^{(1)}(t), q_2^{(1)}(t), \ldots, q_n^{(1)}(t)]^{\mathrm{T}} \tag{13}$$

$$\mathbf{\Phi}_2(x) = [\phi_1^{(2)}(x), \phi_2^{(2)}(x), \ldots, \phi_n^{(2)}(x)], \quad \mathbf{q}_2(t) = [q_1^{(2)}(t), q_2^{(2)}(t), \ldots, q_n^{(2)}(t)]^{\mathrm{T}} \tag{14}$$

where $\mathbf{\Phi}_1(x)$ and $\mathbf{\Phi}_2(x)$ assume the mode functions of boundary-fixed cantilever beam in X and Y directions, respectively. The elements of $\mathbf{\Phi}_1(x)$ and $\mathbf{\Phi}_2(x)$ are given by

$$\phi_i^{(1)}(x) = \sin\frac{(2i-1)\pi}{2L}x, \quad i = 1, 2, \ldots, n \tag{15}$$

$$\phi_i^{(2)}(x) = \cos\,\beta_i x - \cosh\,\beta_i x + \gamma_i(\sin\,\beta_i x - \sinh\,\beta_i x), \quad i = 1, 2, \ldots, n \tag{16}$$

where

$$\beta_1 L = 1.875, \quad \beta_2 L = 4.694, \quad \beta_i L = (i - 0.5)\pi, \quad i \geqslant 3 \tag{17}$$

$$\gamma_i = -\frac{\cos\,\beta_i L + \cosh\,\beta_i L}{\sin\,\beta_i L + \sinh\,\beta_i L} \tag{18}$$

From Eq. (12), the variations δw_1 and δw_2 can be written as

$$\delta w_1 = \mathbf{\Phi}_1 \delta\mathbf{q}_1, \quad \delta w_2 = \mathbf{\Phi}_2 \delta\mathbf{q}_2 \tag{19}$$

The variation of the second-order coupling term $w_c(x, t)$ in Eq. (2) is given by

$$\delta w_c = -\delta\mathbf{q}_2^{\mathrm{T}}\mathbf{S}(x)\mathbf{q}_2 \tag{20}$$

where $\mathbf{S}(x)$ is coupling shape function which is an $n \times n$ vector, given by

$$\mathbf{S}(x) = \int_0^x \mathbf{\Phi}'^{\mathrm{T}}_2(\xi)\mathbf{\Phi}'_2(\xi)\,\mathrm{d}\xi \tag{21}$$

Discretizing Eqs. (7)–(9) and arranging the results, we have

$$\begin{bmatrix} J_H + M_{\theta\theta} & \mathbf{M}_{\theta q_1} & \mathbf{M}_{\theta q_2} \\ \mathbf{M}_{q_1\theta} & \mathbf{M}_{q_1 q_1} & \mathbf{0} \\ \mathbf{M}_{q_2\theta} & \mathbf{0} & \mathbf{M}_{q_2 q_2} \end{bmatrix} \begin{bmatrix} \ddot{\theta} \\ \ddot{\mathbf{q}}_1 \\ \ddot{\mathbf{q}}_2 \end{bmatrix} + 2\dot{\theta} \begin{bmatrix} 0 & \mathbf{0} & \mathbf{0} \\ \mathbf{0} & \mathbf{0} & \mathbf{G}_{q_1 q_2} \\ \mathbf{0} & \mathbf{G}_{q_2 q_1} & \mathbf{0} \end{bmatrix} \begin{bmatrix} \dot{\theta} \\ \dot{\mathbf{q}}_1 \\ \dot{\mathbf{q}}_2 \end{bmatrix} + \begin{bmatrix} 0 & \mathbf{0} & \mathbf{0} \\ \mathbf{0} & \mathbf{K}_{q_1 q_1} & \mathbf{0} \\ \mathbf{0} & \mathbf{0} & \mathbf{K}_{q_2 q_2} \end{bmatrix} \begin{bmatrix} \theta \\ \mathbf{q}_1 \\ \mathbf{q}_2 \end{bmatrix} = \begin{bmatrix} Q_\theta \\ \mathbf{Q}_{q_1} \\ \mathbf{0} \end{bmatrix} + \begin{bmatrix} \tau \\ \mathbf{0} \\ \mathbf{0} \end{bmatrix} \tag{22}$$

where $M_{\theta\theta}$ is the rotary inertia of the beam that is a scalar, and $J_H + M_{\theta\theta}$ is the total rotary inertia of the system; $\mathbf{M}_{q_1 q_1} = \mathbf{M}_1$ and $\mathbf{M}_{q_2 q_2} = \mathbf{M}_2$, where $\mathbf{M}_1$ and $\mathbf{M}_2$ are the $n \times n$ generalized elastic mass matrices of the beam; $\mathbf{M}_{\theta q_1} = \mathbf{M}_{q_1\theta}^{\mathrm{T}}$ and $\mathbf{M}_{\theta q_2} = \mathbf{M}_{q_2\theta}^{\mathrm{T}}$ are $1 \times n$ vectors representing the inertia vectors caused by nonlinear coupling between large rotating motion and elastic deformation; both $\mathbf{G}_{q_1 q_2}$ and $\mathbf{G}_{q_2 q_1}$ are $n \times n$ matrices resulting from the gyroscopic effect; both $\mathbf{K}_{q_1 q_1}$ and $\mathbf{K}_{q_2 q_2}$ are $n \times n$ stiffness matrices; Q_θ is a scalar and $\mathbf{Q}_{q_1}$ is an $n \times 1$ vector, both are the inertia force parameters. All the parameters in Eq. (22) are given as follows:

$$M_{\theta\theta} = J_1 + \mathbf{q}_1^{\mathrm{T}}\mathbf{M}_1\mathbf{q}_1 + \mathbf{q}_2^{\mathrm{T}}\mathbf{M}_2\mathbf{q}_2 + 2(r_A\mathbf{U}_{01} + \mathbf{U}_{11})\mathbf{q}_1 - \underline{\mathbf{q}_2^{\mathrm{T}}(r_A\mathbf{D}_0 + \mathbf{D}_1)\mathbf{q}_2} \tag{23}$$

$$\mathbf{M}_{q_1\theta} = \mathbf{M}_{\theta q_1}^{\mathrm{T}} = -\mathbf{R}\,\mathbf{q}_2 \tag{24}$$

$$\mathbf{M}_{\theta q_2} = \mathbf{M}_{q_2\theta}^{\mathrm{T}} = r_A\mathbf{U}_{02} + \mathbf{U}_{12} + \mathbf{q}_1^{\mathrm{T}}\mathbf{R} \tag{25}$$

$$\mathbf{M}_{q_1 q_1} = \mathbf{M}_1 = \int_0^L \rho A \boldsymbol{\Phi}_1^{\mathrm{T}}\boldsymbol{\Phi}_1 \,\mathrm{d}x \tag{26}$$

$$\mathbf{M}_{q_2 q_2} = \mathbf{M}_2 = \int_0^L \rho A \boldsymbol{\Phi}_2^{\mathrm{T}}\boldsymbol{\Phi}_2 \,\mathrm{d}x \tag{27}$$

$$\mathbf{G}_{q_1 q_2} = -\mathbf{G}_{q_2 q_1}^{\mathrm{T}} = -\mathbf{R} \tag{28}$$

$$\mathbf{K}_{q_1 q_1} = \mathbf{K}_1 - \dot{\theta}^2\mathbf{M}_1 \tag{29}$$

$$\mathbf{K}_{q_2 q_2} = \mathbf{K}_2 - \dot{\theta}^2\mathbf{M}_2 + \underline{\dot{\theta}^2(r_A\mathbf{D}_0 + \mathbf{D}_1)} \tag{30}$$

$$Q_\theta = -2\dot{\theta}[(\mathbf{q}_1^{\mathrm{T}}\mathbf{M}_1\dot{\mathbf{q}}_1 + \mathbf{q}_2^{\mathrm{T}}\mathbf{M}_2\dot{\mathbf{q}}_2) + (r_A\mathbf{U}_{01} + \mathbf{U}_{11})\dot{\mathbf{q}}_1 - \underline{\mathbf{q}_2^{\mathrm{T}}(r_A\mathbf{D}_0 + \mathbf{D}_1)\dot{\mathbf{q}}_2}] \tag{31}$$

$$\mathbf{Q}_{q_1} = \dot{\theta}^2(r_A\mathbf{U}_{01}^{\mathrm{T}} + \mathbf{U}_{11}^{\mathrm{T}}) \tag{32}$$

where $\mathbf{K}_1$ and $\mathbf{K}_2$ in Eqs. (29) and (30) are the $n \times n$ generalized elastic stiffness matrices of the beam. It should be mentioned that the traditional ZOAC model is established based on small deformation assumption in structural dynamics, and it assumes that axial and transverse displacements of the flexible beam are uncoupled, so the obtained dynamics equation will not contain the underlined terms in Eqs. (23), (30) and (31); and also $\mathbf{S}(x) = \mathbf{0}$. In Eq. (30), the underlined term is called *the additional stiffness* term [10,13]. It is the additional stiffness term that is neglected in the traditional ZOAC model, which results in a wrong solution when the beam is in high rotation speed [10,13].

The constant parameters in Eqs. (23)–(32) are given as follows:

$$J_1 = \int_0^L \rho A(r_A + x)^2 \, \mathrm{d}x \tag{33}$$

$$\mathbf{K}_1 = \int_0^L EA\boldsymbol{\Phi}_1'^{\mathrm{T}}\boldsymbol{\Phi}_1' \, \mathrm{d}x \tag{34}$$

$$\mathbf{K}_2 = \int_0^L EI\boldsymbol{\Phi}_2''^{\mathrm{T}}\boldsymbol{\Phi}_2'' \, \mathrm{d}x \tag{35}$$

$$\mathbf{U}_{0j} = \int_0^L \rho A\boldsymbol{\Phi}_j \, \mathrm{d}x, \quad j = 1, 2 \tag{36}$$

$$\mathbf{U}_{1j} = \int_0^L \rho Ax\boldsymbol{\Phi}_j \, \mathrm{d}x, \quad j = 1, 2 \tag{37}$$

$$\mathbf{D}_0 = \int_0^L \rho A\mathbf{S}(x) \, \mathrm{d}x \tag{38}$$

$$\mathbf{D}_1 = \int_0^L \rho Ax\mathbf{S}(x) \, \mathrm{d}x \tag{39}$$

$$\mathbf{R} = \int_0^L \rho A\boldsymbol{\Phi}_1^{\mathrm{T}}\boldsymbol{\Phi}_2 \, \mathrm{d}x \tag{40}$$

where J_1 is a scalar; $\mathbf{U}_{0j}$ and $\mathbf{U}_{1j}$ are both $1 \times n$ vectors; $\mathbf{D}_0$, $\mathbf{D}_1$ and $\mathbf{R}$ are all $n \times n$ matrices.

Eq. (22) may be written in the following matrix form:

$$\mathbf{M}\ddot{\mathbf{Y}} + 2\dot{\theta}\mathbf{G}\dot{\mathbf{Y}} + \mathbf{K}\mathbf{Y} = \mathbf{Q} + \mathbf{F} \tag{41}$$

where $\mathbf{Y}$ is a $(2n+1) \times 1$ vector; $\mathbf{M}$, $\mathbf{G}$ and $\mathbf{K}$ are all $(2n+1) \times (2n+1)$ matrices; $\mathbf{Q}$ and $\mathbf{F}$ are both $(2n+1) \times 1$ vectors; given by

$$\mathbf{Y} = \begin{bmatrix} \theta \\ \mathbf{q}_1 \\ \mathbf{q}_2 \end{bmatrix}, \quad \mathbf{M} = \begin{bmatrix} J_H + M_{\theta\theta} & \mathbf{M}_{\theta q_1} & \mathbf{M}_{\theta q_2} \\ \mathbf{M}_{q_1\theta} & \mathbf{M}_{q_1 q_1} & 0 \\ \mathbf{M}_{q_2\theta} & \mathbf{0} & \mathbf{M}_{q_2 q_2} \end{bmatrix}, \quad \mathbf{G} = \begin{bmatrix} 0 & \mathbf{0} & 0 \\ \mathbf{0} & \mathbf{0} & \mathbf{G}_{q_1 q_2} \\ \mathbf{0} & \mathbf{G}_{q_2 q_1} & \mathbf{0} \end{bmatrix}, \quad \mathbf{K} = \begin{bmatrix} 0 & \mathbf{0} & \mathbf{0} \\ \mathbf{0} & \mathbf{K}_{q_1 q_1} & \mathbf{0} \\ \mathbf{0} & \mathbf{0} & \mathbf{K}_{q_2 q_2} \end{bmatrix},$$

$$\mathbf{Q} = \begin{bmatrix} Q_\theta \\ \mathbf{Q}_{q_1} \\ \mathbf{0} \end{bmatrix}, \quad \mathbf{F} = \begin{bmatrix} \tau \\ \mathbf{0} \\ \mathbf{0} \end{bmatrix} \tag{42}$$

2.3. Effect of damping

Damping in flexible hub–beam system has important effect on dynamic characteristics, especially for the case with high-speed large motion or large deformation of the beam. In past studies on flexible hub–beam system, effect of damping is often not considered in the modelling. In this paper, this effect is taken into account, and it will be demonstrated numerically in Section 4 that damping may have great effect on system dynamics. Three kinds of damping adopted in Ref. [10] are considered herein: structural damping of beam material, air damping caused by rotational motion of the beam, and damping located at the hub bearing caused by rotational motion of the hub. Damping of beam material is assumed to be the viscous damping similar to that in structural dynamics. For air damping, viscous damping and square damping are considered,

respectively. Damping of the hub bearing is assumed to be viscous too. Contributions of damping to dynamic equation are given blow.

Structural damping of the flexible beam may be determined by the mass coefficient method in structural dynamics. In consideration of different damping of the beam in axial and transverse directions, structural damping matrix of the beam may be written as

$$\mathbf{C}_1 = \begin{bmatrix} 0 & \mathbf{0} & \mathbf{0} \\ \mathbf{0} & \alpha_1\mathbf{M}_1 & \mathbf{0} \\ \mathbf{0} & \mathbf{0} & \alpha_2\mathbf{M}_2 \end{bmatrix} \tag{43}$$

where $\mathbf{C}_1$ is a $(2n+1)\times(2n+1)$ matrix; α_1 and α_2 are the damping coefficients of the beam in axial and transverse directions, respectively. The parameters $\mathbf{M}_1$ and $\mathbf{M}_2$ are given in Eqs. (26) and (27).

When the beam moves in air, air resistance occurs and it causes the air damping force. As pointed out in Refs. [10,14], two kinds of air damping force may be considered: the viscous damping force proportional to instantaneous velocity and the square damping force proportional to the square of instantaneous velocity. These two air damping forces are considered herein and their contributions to system dynamics are given below.

For the viscous air damping, damping force is proportional to instantaneous velocity. Damping force distributed along the beam may be written as [10,14]

$$\vec{F}_1 = -\beta_1\dot{\vec{r}}_P \tag{44}$$

where β_1 is the viscous damping coefficient. In matrix form, Eq. (44) becomes

$$\mathbf{F}_1 = -\beta_1[\dot{\mathbf{r}}_A + \dot{\mathbf{\Theta}}(\mathbf{r}_0 + \mathbf{r}_1) + \mathbf{\Theta}\dot{\mathbf{r}}_1] \tag{45}$$

When virtual displacement of the beam is produced, the virtual work δW_1 done by the viscous damping force $\mathbf{F}_1$ may be written as

$$\delta W_1 = -\beta_1 \int_0^L \delta\mathbf{r}_P^{\mathrm{T}}[\dot{\mathbf{r}}_A + \dot{\mathbf{\Theta}}(\mathbf{r}_0 + \mathbf{r}_1) + \mathbf{\Theta}\dot{\mathbf{r}}_1]\,\mathrm{d}x \tag{46}$$

Expanding Eq. (46) and then substituting the result into the expression of the Hamilton theory $\int_{t_1}^{t_2}(\delta T - \delta H + \delta W_F)\,\mathrm{d}t = 0$, we find that the contribution of the viscous air damping to dynamic equation is a damping matrix, given by

$$\mathbf{C}_2 = \frac{\beta_1}{\rho A}\begin{bmatrix} M_{\theta\theta} & \mathbf{M}_{\theta q_1} & \mathbf{M}_{\theta q_2} \\ \mathbf{M}_{q_1\theta} & \mathbf{M}_{q_1 q_1} & \mathbf{0} \\ \mathbf{M}_{q_2\theta} & \mathbf{0} & \mathbf{M}_{q_2 q_2} \end{bmatrix} \tag{47}$$

It is observed from Eq. (47) that, the damping matrix $\mathbf{C}_2$ has similar structure with the mass matrix in Eq. (22), but the first element of $\mathbf{C}_2$ does not contain the rotary inertia of the hub, J_H. All parameters in Eq. (47) are shown in Eqs. (23)–(27).

If rotating velocity of the beam is high or deformation of the beam is large, damping force caused by the air is generally taken to be proportional to the square of absolute instantaneous velocity, thus damping force distributed along the beam may be written as [10,14]

$$\vec{F}_2 = -\beta_2\dot{\vec{r}}_P\left|\dot{\vec{r}}_P\right| \tag{48}$$

where β_2 is the square damping coefficient and $\left|\dot{\vec{r}}_P\right| \geqslant 0$ is a scalar. In matrix form, Eq. (48) is written as

$$\mathbf{F}_2 = -\beta_2[\dot{\mathbf{r}}_A + \dot{\mathbf{\Theta}}(\mathbf{r}_0 + \mathbf{r}_1) + \mathbf{\Theta}\dot{\mathbf{r}}_1]\left|\dot{\mathbf{r}}_A + \dot{\mathbf{\Theta}}(\mathbf{r}_0 + \mathbf{r}_1) + \mathbf{\Theta}\dot{\mathbf{r}}_1\right| \tag{49}$$

It is observed from Eq. (49) that the square damping force is complex in expression and it causes analytical complexity to the solution of dynamic equation as well. One treatment to this problem is to make some

predigestion for Eq. (49). For a slender beam with high rotation, effects of $\mathbf{r}_1$ and $\dot{\mathbf{r}}_1$ in the sign $|\cdot|$ in Eq. (49) may reasonably be neglected [10], so Eq. (49) becomes

$$\mathbf{F}_2 \approx -\beta_2[\dot{\mathbf{r}}_A + \dot{\boldsymbol{\Theta}}(\mathbf{r}_0 + \mathbf{r}_1) + \boldsymbol{\Theta}\dot{\mathbf{r}}_1]|\dot{\mathbf{r}}_A + \mathbf{r}\ddot{\boldsymbol{\Theta}}_0| \tag{50}$$

Similar to the deduction of damping matrix $\mathbf{C}_2$, contribution of the square damping force to dynamic equation is also a damping matrix, given by

$$\mathbf{C}_3 = \frac{\beta_2\dot{\theta}\,\mathrm{sign}(\dot{\theta})}{\rho A}\begin{bmatrix} C_{11} & \mathbf{C}_{21}^{\mathrm{T}} & \mathbf{C}_{31}^{\mathrm{T}} \\ \mathbf{C}_{21} & \mathbf{C}_{22} & \mathbf{0} \\ \mathbf{C}_{31} & \mathbf{0} & \mathbf{C}_{33} \end{bmatrix} \tag{51}$$

where C_{11} is a scalar, $\mathbf{C}_{21}$ and $\mathbf{C}_{31}$ are both $n\times 1$ vectors, $\mathbf{C}_{22}$ and $\mathbf{C}_{33}$ are both $n\times n$ matrices, given by

$$\begin{aligned} C_{11} = {} & \int_0^L \rho A(r_A + x)^3\,\mathrm{d}x + \mathbf{q}_1^{\mathrm{T}}\left[r_A\mathbf{M}_1 + \int_0^L \rho A x\boldsymbol{\Phi}_1^{\mathrm{T}}\boldsymbol{\Phi}_1\,\mathrm{d}x\right]\mathbf{q}_1 + \mathbf{q}_2^{\mathrm{T}}\left[r_A\mathbf{M}_2 + \int_0^L \rho A x\boldsymbol{\Phi}_2^{\mathrm{T}}\boldsymbol{\Phi}_2\,\mathrm{d}x\right]q_2 \\ & + 2\left[r_A^2\mathbf{U}_{01} + 2r_A\mathbf{U}_{11} + \int_0^L \rho A x^2\boldsymbol{\Phi}_1\,\mathrm{d}x\right]\mathbf{q}_1 - \underline{\mathbf{q}_2^{\mathrm{T}}\left[r_A^2\mathbf{D}_0 + 2r_A\mathbf{D}_1 + \int_0^L \rho A x^2\mathbf{S}(x)\,\mathrm{d}x\right]\mathbf{q}_2} \end{aligned} \tag{52}$$

$$\mathbf{C}_{21} = -\left[r_A\mathbf{R} + \int_0^L \rho A x\boldsymbol{\Phi}_1^{\mathrm{T}}\boldsymbol{\Phi}_2\,\mathrm{d}x\right]\mathbf{q}_2 \tag{53}$$

$$\mathbf{C}_{31} = r_A^2\mathbf{U}_{02}^{\mathrm{T}} + 2r_A\mathbf{U}_{12}^{\mathrm{T}} + \int_0^L \rho A x^2\boldsymbol{\Phi}_2^{\mathrm{T}}\,\mathrm{d}x + \left[r_A\mathbf{R} + \int_0^L \rho A x\boldsymbol{\Phi}_2^{\mathrm{T}}\boldsymbol{\Phi}_1\,\mathrm{d}x\right]\mathbf{q}_1 \tag{54}$$

$$\mathbf{C}_{22} = r_A\mathbf{M}_1 + \int_0^L \rho A x\boldsymbol{\Phi}_1^{\mathrm{T}}\boldsymbol{\Phi}_1\,\mathrm{d}x \tag{55}$$

$$\mathbf{C}_{33} = r_A\mathbf{M}_2 + \int_0^L \rho A x\boldsymbol{\Phi}_2^{\mathrm{T}}\boldsymbol{\Phi}_2\,\mathrm{d}x \tag{56}$$

where $\mathbf{M}_1$ and $\mathbf{M}_2$ are shown in Eqs. (26) and (27); $\mathbf{U}_{0j}$, $\mathbf{U}_{1j}$, $\mathbf{D}_0$, $\mathbf{D}_1$ and $\mathbf{R}$ are shown in Eqs. (36)–(40), $j = 1,2$; $\mathbf{S}(x)$ is shown in Eq. (21). The underlined term in Eq. (52) results from the consideration of coupling term of deformation of the beam.

Synthetize the above damping and consider the viscous damping of hub bearing, the total damping matrix of the system may be written as

$$\mathbf{C}_t = \begin{bmatrix} C_H & \mathbf{0} & \mathbf{0} \\ \mathbf{0} & \alpha_1\mathbf{M}_1 & \mathbf{0} \\ \mathbf{0} & \mathbf{0} & \alpha_2\mathbf{M}_2 \end{bmatrix} + \frac{\beta_1}{\rho A}\begin{bmatrix} M_{\theta\theta} & \mathbf{M}_{\theta q_1} & \mathbf{M}_{\theta q_2} \\ \mathbf{M}_{q_1\theta} & \mathbf{M}_{q_1 q_1} & \mathbf{0} \\ \mathbf{M}_{q_2\theta} & \mathbf{0} & \mathbf{M}_{q_2 q_2} \end{bmatrix} + \frac{\beta_2\dot{\theta}\,\mathrm{sign}(\dot{\theta})}{\rho A}\begin{bmatrix} C_{11} & \mathbf{C}_{21}^{\mathrm{T}} & \mathbf{C}_{31}^{\mathrm{T}} \\ \mathbf{C}_{21} & \mathbf{C}_{22} & \mathbf{0} \\ \mathbf{C}_{31} & \mathbf{0} & \mathbf{C}_{33} \end{bmatrix} \tag{57}$$

where C_H is the viscous damping coefficient of the bearing of hub.

Adding the damping matrix given by Eq. (57) into Eq. (41), the dynamic equation considering damping may be obtained as

$$\mathbf{M}\ddot{\mathbf{Y}} + (2\dot{\theta}\mathbf{G} + \mathbf{C}_t)\dot{\mathbf{Y}} + \mathbf{K}\mathbf{Y} = \mathbf{Q} + \mathbf{F} \tag{58}$$

In Eqs. (41) and (58), we call the dynamic model with consideration of the underlined terms in Eqs. (23), (30), (31) and (52) *the FOAC model*, and that without consideration of these underlined terms *the ZOAC model*.

3. Dynamic model in non-inertial system

For dynamic problem of flexible hub–beam system in non-inertial system, the law of large motion is usually assumed known and need not be solved. Dynamic model of flexible hub–beam system in non-inertial system can be obtained by neglecting the equation of large motion in Eq. (22).

3.1. Dynamic equation without damping

Neglecting the first row of equation in Eq. (22), the dynamic model of flexible hub–beam system in non-inertial system without damping can be written as

$$\begin{bmatrix} \mathbf{M}_1 & \mathbf{0} \\ \mathbf{0} & \mathbf{M}_2 \end{bmatrix} \begin{bmatrix} \ddot{\mathbf{q}}_1 \\ \ddot{\mathbf{q}}_2 \end{bmatrix} + 2\dot{\theta} \begin{bmatrix} \mathbf{0} & \mathbf{G}_{q_1q_2} \\ \mathbf{G}_{q_2q_1} & \mathbf{0} \end{bmatrix} \begin{bmatrix} \dot{\mathbf{q}}_1 \\ \dot{\mathbf{q}}_2 \end{bmatrix} + \begin{bmatrix} \mathbf{K}_{q_1q_1} & \mathbf{0} \\ \mathbf{0} & \mathbf{K}_{q_2q_2} \end{bmatrix} \begin{bmatrix} \mathbf{q}_1 \\ \mathbf{q}_2 \end{bmatrix} = \begin{bmatrix} \mathbf{Q}_{q_1} \\ \mathbf{0} \end{bmatrix} - \ddot{\theta} \begin{bmatrix} \mathbf{M}_{q_1\theta} \\ \mathbf{M}_{q_2\theta} \end{bmatrix} \tag{59}$$

All parameters in Eq. (59) are shown in Eqs. (24)–(30) and (32).

3.2. Dynamic equation with damping

If damping is considered, the dynamic equation of the system in non-inertial system may be written as

$$\begin{bmatrix} \mathbf{M}_1 & \mathbf{0} \\ \mathbf{0} & \mathbf{M}_2 \end{bmatrix} \begin{bmatrix} \ddot{\mathbf{q}}_1 \\ \ddot{\mathbf{q}}_2 \end{bmatrix} + \dot{\theta} \begin{bmatrix} \mathbf{C}_{t_1} & 2\mathbf{G}_{q_1q_2} \\ 2\mathbf{G}_{q_2q_1} & \mathbf{C}_{t_2} \end{bmatrix} \begin{bmatrix} \dot{\mathbf{q}}_1 \\ \dot{\mathbf{q}}_2 \end{bmatrix} + \begin{bmatrix} \mathbf{K}_{q_1q_1} & \mathbf{0} \\ \mathbf{0} & \mathbf{K}_{q_2q_2} \end{bmatrix} \begin{bmatrix} \mathbf{q}_1 \\ \mathbf{q}_2 \end{bmatrix} = \begin{bmatrix} \mathbf{Q}_{q_1} \\ 0 \end{bmatrix} + \begin{bmatrix} \overline{\mathbf{Q}}_1 \\ \overline{\mathbf{Q}}_2 \end{bmatrix} + \begin{bmatrix} \hat{\mathbf{Q}}_1 \\ \hat{\mathbf{Q}}_2 \end{bmatrix} \tag{60}$$

where $\mathbf{M}_1$, $\mathbf{M}_2$, $\mathbf{G}_{q_1q_2}$, $\mathbf{G}_{q_2q_1}$, $\mathbf{K}_{q_1q_1}$, $\mathbf{K}_{q_2q_2}$, and $\mathbf{Q}_{q_1}$ are shown in Eqs. (26)–(30) and (32). The parameters $\mathbf{C}_{t_1}$ and $\mathbf{C}_{t_2}$ are $n \times n$ matrices; inertial forces $\overline{\mathbf{Q}}_1$ and $\overline{\mathbf{Q}}_2$ are $n \times 1$ vectors; damping forces $\hat{\mathbf{Q}}_1$ and $\hat{\mathbf{Q}}_2$ are $n \times 1$ vectors; which are given by

$$\mathbf{C}_{t_1} = \left(\alpha_1 + \frac{\beta_1}{\rho A}\right)\mathbf{M}_1 + \frac{\beta_2 \dot{\theta}\,\mathrm{sign}(\dot{\theta})}{\rho A}\mathbf{C}_{22} \tag{61}$$

$$\mathbf{C}_{t_2} = \left(\alpha_2 + \frac{\beta_1}{\rho A}\right)\mathbf{M}_2 + \frac{\beta_2 \dot{\theta}\,\mathrm{sign}(\dot{\theta})}{\rho A}\mathbf{C}_{33} \tag{62}$$

$$\overline{\mathbf{Q}}_1 = -\ddot{\theta}\mathbf{M}_{q_1\theta} \tag{63}$$

$$\overline{\mathbf{Q}}_2 = -\ddot{\theta}\mathbf{M}_{q_2\theta} \tag{64}$$

$$\hat{\mathbf{Q}}_1 = -\left(\frac{\beta_1 \dot{\theta}}{\rho A}\mathbf{M}_{q_1\theta} + \frac{\beta_2 \dot{\theta}^2\,\mathrm{sign}(\dot{\theta})}{\rho A}\mathbf{C}_{21}\right) \tag{65}$$

$$\hat{\mathbf{Q}}_2 = -\left(\frac{\beta_1 \dot{\theta}}{\rho A}\mathbf{M}_{q_2\theta} + \frac{\beta_2 \dot{\theta}^2\,\mathrm{sign}(\dot{\theta})}{\rho A}\mathbf{C}_{31}\right) \tag{66}$$

where $\mathbf{C}_{21}$, $\mathbf{C}_{31}$, $\mathbf{C}_{22}$, and $\mathbf{C}_{33}$ are shown in Eqs. (53)–(56), respectively.

In Eqs. (59) and (60), we also call the dynamic model with the underlined term in Eq. (30) the FOAC model, and that without the underlined term the ZOAC model.

4. Numerical simulations

In this section, validity of the proposed dynamic models is verified by numerical simulations. Two cases are considered: (1) dynamics in non-inertial system with known large motion of system and (2) dynamics with

unknown large motion of system. The two structural models adopted in Ref. [10] are used herein for simulations. In Ref. [10], FEM is used as the discretization method for flexible hub–beam system.

4.1. Dynamics in a non-inertial system

Here, we consider dynamic characteristics in non-inertial system of the hub–beam system. The structural model is shown in Fig. 1 where $r_A = 0.55\,\mathrm{m}$. Properties of the flexible beam are taken as the same as those in Ref. [10], and given as follows. The length of beam is $L = 0.9\,\mathrm{m}$, the thickness is 0.001 m and the height is 0.0318 m, the cross-sectional area of beam is $A = 3.18 \times 10^{-5}\,\mathrm{m}^2$ and the area moment of inertia of beam cross-section is $I = 2.65 \times 10^{-12}\,\mathrm{m}^4$. The mass density of the beam is $\rho = 7.866 \times 10^3\,\mathrm{kg/m}^3$; and the modulus of elasticity is $E = 2.01 \times 10^{11}\,\mathrm{N/m}^2$. The rotary inertia of hub is about $J_H = 11.8\,\mathrm{kg\,m}^2$ and that of beam is about $0.2\,\mathrm{kg\,m}^2$. Since the rotary inertia of hub is much larger than that of beam, vibration motion of beam has very small effect on the rotation motion of hub. The law of large rotation motion of the system adopted in Ref. [10] is used herein, given by

$$\dot{\theta} = \begin{cases} \omega_0(1 - \mathrm{e}^{-(5t/T_0)})/(1 - \mathrm{e}^{-(20/3)}), & 0 \leqslant t \leqslant T \\ \omega_0, & t > T \end{cases} \tag{67}$$

where $T_0 = 60\,\mathrm{s}$, $T = 80\,\mathrm{s}$, and $\omega_0 = 3.46\,\mathrm{rad/s}$. The angular velocity of beam reaches ω_0 at $T = 80\,\mathrm{s}$. The law of large rotation motion is shown in Fig. 3.

Here, the structural damping coefficient is referred to Ref. [10], i.e., $\alpha_1 = \alpha_2 = 0.011$. Two kinds of air damping may be caused by large motion of the beam: viscous damping and square damping. It was pointed out in Refs. [10,14] that, in past experimental studies, no evidence shows that these two type of air damping appear simultaneously in the system or there exists a critical rotation velocity which makes damping convert from one form to another one. It was also indicated in Refs. [10,14] that the square air damping plays key role for the case of high-speed motion. Therefore, the square air damping proportional to the square of instantaneous velocity is considered in this simulation. The square damping coefficient β_2 may be determined according to the following established equation [10,14]:

$$\beta_2 = \tfrac{1}{2}\rho_A C_d W_s, \quad C_d = 5.63 S^{1/3} \tag{68}$$

where ρ_A is the density of air, C_d the established coefficient, S the air-faced area, and W_s the width of air-faced surface.

The value $\beta_2 = 0.0353$ is chosen as that in Ref. [10]. The viscous damping coefficient β_1 is set to zero, i.e., $\beta_1 = 0$. In experimental studies of flexible hub–beam system in Ref. [10], an air bearing is installed in the hub such that the hub–beam system may suspend in air. So the damping located at the air bearing is very small and may be neglected, namely $C_H = 0$ is taken in Eq. (57). It should be mentioned herein that, validity of the FOAC model is verified through experiment to the above structural model in Ref. [10], in which FEM is used as discretization method and the above physical parameters are taken. For the structural model considered

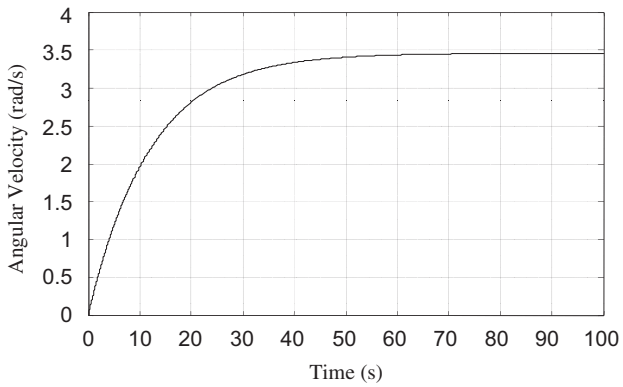

Fig. 3. Time history of angular velocity of large motion of system.

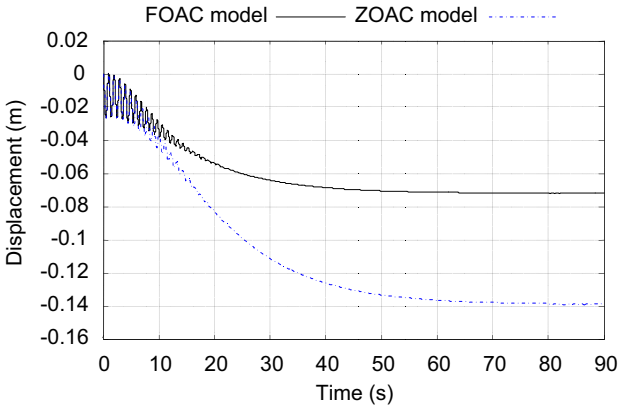

Fig. 4. Tip response of beam in the Y direction with damping.

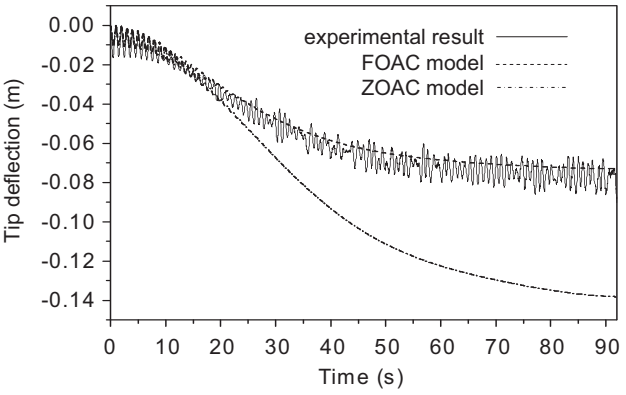

Fig. 5. Experimental and simulation results using FEM in Ref. [10].

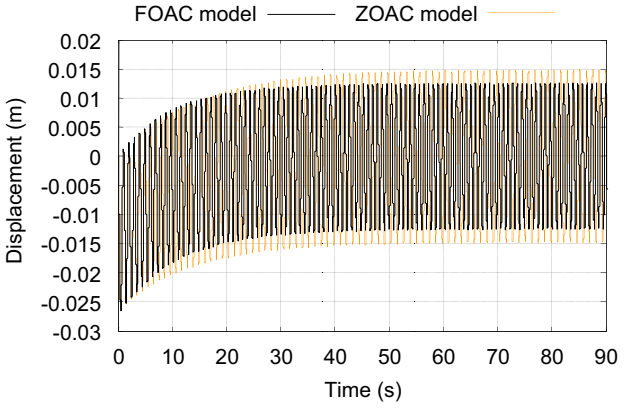

Fig. 6. Tip response of beam in the Y direction without damping.

herein, all physical and structural parameters are referred to Ref. [10], except that AMM is used as discretization method for dynamic equation of the system. For this condition, validity of AMM may be verified by comparing simulation results of AMM with that of FEM. In the numerical simulations below, the first two modes of the beam is used when using AMM.

Under the large motion law given in Eq. (67), the tip responses of beam in Y direction by using the ZOAC and FOAC models are displayed in Fig. 4, respectively, where the solid line is the result using the FOAC model and the dot-dashed line the ZOAC model. It is observed from Fig. 4 that there exists big difference in the two lines, especially for the time after 10 s. The offset quantity of the tip of beam in steady vibration phase when using the FOAC model is about 7 cm, and that when using the ZOAC model is 14 cm which is twice of the case of the FOAC model. The simulation and experimental results obtained in Ref. [10] are scanned and displayed in Fig. 5 for comparison too, in which FEM is used for discretization of dynamic equation. It is observed from the comparison of Figs. 4 and 5 that AMM may achieve almost the same result as FEM. This indicates the validity of AMM presented in this paper. In the simulations for Figs. 4 and 5, the structural damping and the square air damping are considered. If the two damping are neglected in dynamic equation, namely $\alpha_1 = \alpha_2 = \beta_2 = 0$ are taken, the results are shown in Fig. 6 which shows a high-frequency vibration. A comparison of Fig. 6 with Figs. 4 and 5 indicates that damping has great effect on system dynamics. Because high-frequency vibration occurs in Fig. 6, so vibration amplitude of the beam in Fig. 6 without damping is smaller than that in Fig. 4 with damping.

In past simulations and experimental studies, damping is usually not considered in the modelling, or structural damping is considered with air damping neglected. When difference occurs between simulation and experimental results, more attention is focused on numerical algorithm and model veracity to solve this difference. Air damping is herein studied to demonstrate that it affects dynamic behaviour of the system greatly in some cases. The result with only structural damping and neglecting air damping in the dynamic equation is shown in Fig. 7. It again shows a high-frequency vibration. It is observed from Figs. 4 and 7 that there exists significant difference in the results with and without air damping.

It is observed from the simulations above that there exists significant difference between the results using the ZOAC and FOAC models. To further reveal the difference of these two dynamic models, the law of large motion adopted in Refs. [3,15,16], cited by many studies, is used for the structural model. In the studies using this law, all damping is often not taken into account. Therefore, damping is also not considered in the simulations below. The law of large motion is given by

$$\dot{\theta} = \begin{cases} \dfrac{\omega_0}{T}t - \dfrac{\omega_0}{2\pi}\sin\left(\dfrac{2\pi}{T}t\right), & 0 \leqslant t \leqslant T \\ \omega_0, & t > T \end{cases} \tag{69}$$

where $T = 15$ s and $\omega_0 = 3.46$ rad/s. The beam reaches an angular velocity ω_0 at $T = 15$ s and then rotates at a constant angular velocity of ω_0. According to the law given in Eq. (69), the simulation results are displayed in Fig. 8, where Fig. 8(b) is the magnified figure of Fig. 8(a) when $15 \leqslant t \leqslant 20$. As observed in Fig. 8(a), the maximum transverse displacement of beam using the traditional ZOAC model is larger than that of the FOAC model in the accelerating phase of motion. It is also observed in Fig. 8(b) that the beam behaves with a periodical vibration at the phase of steady motion. In this phase, the vibration amplitude of the ZOAC model

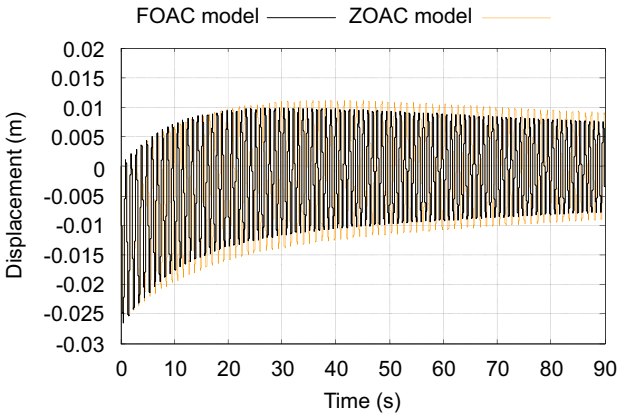

Fig. 7. Tip response of beam in the Y direction with structural damping and without wind damping.

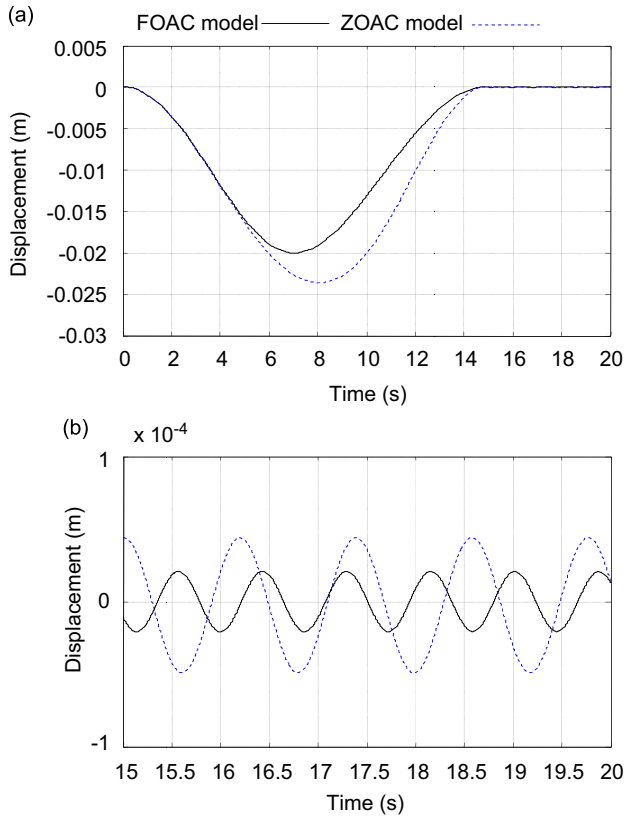

Fig. 8. Tip response of beam in the Y direction without damping and using Kane's angular velocity.

is larger than that of the FOAC model, but the vibration frequency is otherwise. In the steady phase, the fundamental frequency of tip vibration of beam in Y direction by the FOAC model is 1.163 Hz, and that by the ZOAC model is 0.841 Hz. For the flexible cantilever beam without large motion, the fundamental frequency is 1.006 Hz. We observe that the transverse vibration frequency of the beam by the FOAC model is increased in comparison with that without large motion and it shows a "dynamic stiffening" phenomenon. On the contrary, the transverse vibration frequency by the ZOAC model is smaller than that without large motion and it shows a "softening" phenomenon. The "softening" phenomenon is a result of the neglect of dynamic stiffness term related with the coupling deformation of the beam.

4.2. Studies of rigid–flexible coupling dynamics

We observe from the simulations above that the presence of damping in the modelling is significant and incorrect result may be obtained if damping is not considered. In the following simulation, the method above is introduced to consider cases that large motion of the system is unknown.

In the studies above for dynamics in non-inertial system, the law of large motion of system is assumed known. This case neglects the effect of elastic vibration of the beam in large motion of the system. For practical rigid–flexible coupling dynamic systems, the law of external forces acted on the system is usually known, but the law of large motion of the system is unknown, which is to be solved from the known conditions. The large motion of the system causes elastic vibration of the flexible beam, which, in turn, affects the large motion of the system. These two motions act on each other. The case of unknown large motion of system is studied here. The radius of the hub is assumed to be $r_A = 0.05\,\mathrm{m}$, and its rotary inertia is $J_H = 0.30\,\mathrm{kg\,m^2}$. The properties of the flexible beam are given as follows. The length is $L = 1.8\,\mathrm{m}$; the cross-sectional area is $A = 2.5 \times 10^{-4}\,\mathrm{m^2}$; the area moment of inertia of beam cross-section is $I = 1.3021 \times 10^{-10}\,\mathrm{m^4}$;

the mass density is $\rho = 2.766 \times 10^3\,\mathrm{kg/m^3}$; and the modulus of elasticity is $E = 6.90 \times 10^{10}\,\mathrm{N/m^2}$. The rotary inertia of beam is about $1.46\,\mathrm{kg\,m^2}$, which is much larger than that of hub.

Here, we assume the following rotating torque is acted on the hub [10]:

$$\tau(t) = \begin{cases} \tau_0 \sin\left(\dfrac{2\pi}{T}t\right), & 0 \leqslant t \leqslant T \\ 0, & t > T \end{cases} \tag{70}$$

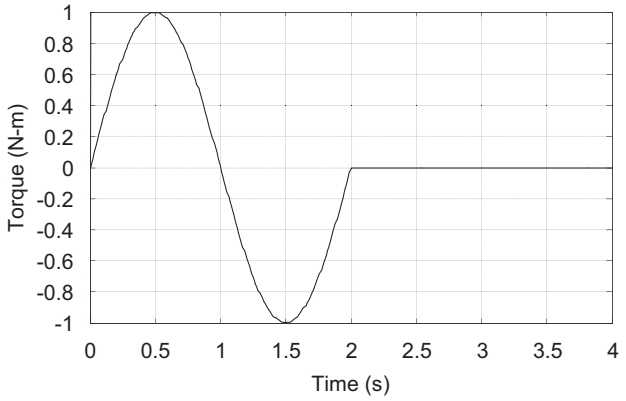

Fig. 9. Time history of external torque.

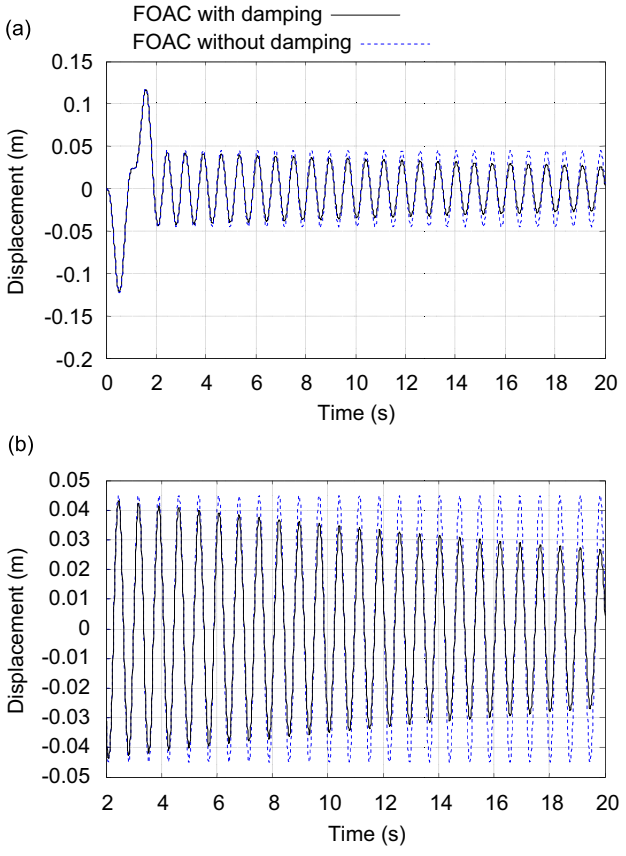

Fig. 10. Tip response of beam with and without damping.

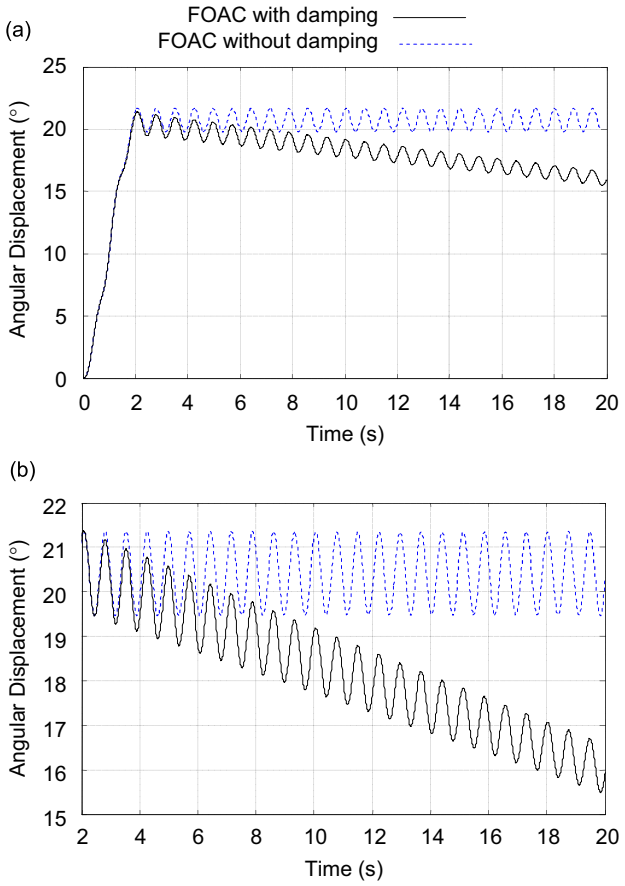

Fig. 11. Time history of angular displacement of beam with and without damping.

where $T = 2$ s. Eq. (70) indicates that the external torque acts on the hub according to the law of the first equation in Eq. (70) when $0 \leqslant t \leqslant T$, and the external torque will be removed when $t > T$. The parameter τ_0 is chosen to be $\tau_0 = 1$ N m. Fig. 9 shows the time history of the external torque given by Eq. (70). The damping coefficients of the system are taken as the same in the last example, i.e., $\alpha_1 = \alpha_2 = 0.011$, $\beta_1 = 0$, $\beta_2 = 0.0353$, and $C_H = 0$. In the following simulation, the first two modes of the beam are adopted again when using the AMM.

In accordance with the law in Eq. (70), the tip responses of the beam in Y direction is displayed in Fig. 10, where the solid line is the result of the FOAC model with damping, and the dashed line without damping. Fig. 10(b) is the magnified figure of Fig. 10(a) when $2 \leqslant t \leqslant 20$. We observe in Fig. 10 that the beam has constant-amplitude vibration in steady vibration phase for the case without damping, and it behaves with a decayed vibration for the case with damping. Fig. 11 shows the time history of angular displacement of the system. Fig. 11(b) is the magnified figure of Fig. 11(a) when $2 \leqslant t \leqslant 20$. If analytical method of multirigidbody dynamics is used, with $J_1\ddot{\theta} = \tau$, we can obtain the time history of angular displacement of the system as a smooth curve with no undulation, and the flexible beam will stay at $\theta = 20.75^\circ$ after large rotating motion. But for the rigid–flexible coupling case without damping, from Figs. 10 and 11 we observe that the beam swings at $\theta = 20.75^\circ$. For the case with damping, the swing motion of hub shows also a decayed motion. Furthermore, it shows a motion trend contrary to the rotation motion of the system.

In conclusion, we observe in Figs. 10 and 11 that damping has significant effect on system dynamics for the rigid–flexible coupling of the hub–beam system.

5. Concluding remark

In this paper, the dynamic characteristics of a flexible hub–beam system with damping effect are investigated using the assumed mode discretization method. Two cases with known and unknown large motion of the system are considered. Three kinds of damping are considered in the modelling: the structural damping of the beam material, the air damping caused by the large motion of the system, and the damping of the hub bearing. For air damping, the viscous damping proportional to the instantaneous velocity, and the square damping proportional to the square of instantaneous velocity are considered. Simulation results indicate that the FOAC model based on AMM is valid for describing the dynamic behaviour of the flexible hub–beam system, whereas the traditional ZOAC model may result in incorrect solutions. When the large motion of the system is in high speed or the flexibility of beam is large, damping in the system has significant effect on system dynamics and should not be disregarded in the modelling.

Acknowledgements

The work described in this paper was supported by a grant from City University of Hong Kong [Project no. 7001875 (BC)], the Science Foundation of China (10772112, 10472065), the Key Project of Ministry of Education of China (107043) and the Specialized Research Fund for the Doctoral Program of Higher Education of China (20070248032).

References

[1] R.P. Singh, R.J. Voor, P.W. Likins, Dynamics of flexible bodies in three-topology: a computer-oriented approach, *Journal of Guidance, Control and Dynamics* 8 (1985) 584–590.
[2] L. Meirovitch, Hybrid state equations of motion for flexible bodies in terms of quasi-coordinates, *Journal of Guidance, Control and Dynamics* 14 (5) (1990) 1374–1383.
[3] T.R. Kane, R.R. Ryan, A.K. Banerjee, Dynamics of a cantilever beam attached to a moving base, *Journal of Guidance, Control and Dynamics* 10 (2) (1987) 139–151.
[4] J. Baillieul, M. Levi, Rotational elastic dynamics, *Physica D* 27 (1987) 43–62.
[5] P.S. Krishnaprasad, J.E. Marsden, Hamiltonian structures and stability for rigid bodies with flexible attachments, *Archive for Rational Mechanics and Analysis* 98 (1) (1987) 71–93.
[6] S. Choura, S. Jayasuriya, M.A. Medick, On the modeling, and openloop control of a rotating thin flexible beam, *Journal of Dynamic Systems, Measurement, and Control—Transactions of the ASME* 113 (1991) 27–33.
[7] D.J. Zhang, R.L. Huston, On dynamic stiffening of flexible bodies having high angular velocity, *Mechanics of Structures and Machines* 24 (3) (1996) 313–329.
[8] J. Mayo, J. Dominguez, A.A. Shabana, Geometrically nonlinear formulation of beam in flexible multibody dynamics, *Journal of Vibration and Acoustics—Transactions of the ASME* 117 (1995) 501–509.
[9] O. Wallrapp, Standardization of flexible body modeling in multibody system codes, part I: definition of standard input data, *Mechanics of Structures and Machines* 22 (3) (1994) 283–304.
[10] Yang Hui, Study of Dynamic Modeling Theory and Experiments for Rigid–Flexible Coupling Systems, PhD Dissertation, Shanghai Jiaotong University, China, 2002 (in Chinese).
[11] Yang Hui, Hong Jia-Zhen, Yu Zheng-Yue, Vibration analysis and experiment investigation for a typical rigid–flexible coupled system, *Chinese Journal of Astronautics* 23 (2) (2002) 67–72 (in Chinese).
[12] Yang Hui, Hong Jia-Zhen, Yu Zheng-Yue, Experiment validation on modelling theory for rigid–flexible coupling systems, *Acta Mechanica Sinica* 35 (2) (2003) 253–256 (in Chinese).
[13] Cai Guo-Ping, Hong Jia-Zhen, Simon X. Yang, Dynamic analysis of a flexible hub–beam system with tip mass, *Mechanics Research Communications* 32 (2) (2005) 173–190.
[14] J.N. Juang, L.G. Horta, Efforts of atmosphere on slewing control of a flexible structure, *Journal of Guidance, Control and Dynamics* 10 (4) (1987) 387–392.
[15] Ryu Jeha, Kim Sung-Sup, Kim Sung-Soo, A general approach to stress stiffening effects on flexible multibody dynamic systems, *Mechanics of Structures and Machines* 22 (2) (1994) 157–180.
[16] S.C. Wu, E.J. Haug, Geometric non-linear substructuring for dynamics of flexible mechanical system, *International Journal of Numerical Methods in Engineering* 26 (1988) 2211–2226.